J. Phys.: Condens. Matter **22** (2010) 455105 (6pp) doi:10.1088/0953-8984/22/45/455105

Equilibrium structure of ferrofluid aggregates

Mina Yoon[1,2] **and David Tománek**[3]

[1] Materials Science and Technology Division, Oak Ridge National Laboratory, Oak Ridge, TN 37831, USA
[2] Fritz-Haber-Institut der Max-Planck-Gesellschaft, Faradayweg 4-6, Berlin 14195, Germany
[3] Physics and Astronomy Department, Michigan State University, East Lansing, MI 48824-2320, USA

Received 22 July 2010, in final form 29 September 2010
Published 28 October 2010
Online at stacks.iop.org/JPhysCM/22/455105

Abstract
We study the equilibrium structure of large but finite aggregates of magnetic dipoles, representing a colloidal suspension of magnetite particles in a ferrofluid. With increasing system size, the structural motif evolves from chains and rings to multi-chain and multi-ring assemblies. Very large systems form single- and multi-wall coils, tubes and scrolls. These structural changes result from a competition between various energy terms, which can be approximated analytically within a continuum model. We also study the effect of external parameters such as magnetic field on the relative stability of these structures. Our results may give insight into experimental data obtained during solidification of ferrofluid aggregates at temperatures where thermal fluctuations become negligible in comparison to inter-particle interactions. These data may also help to experimentally control the aggregation of magnetic particles.

1. Introduction

Complex fluids, consisting of a colloidal suspension of particles carrying electric or magnetic dipole moments [1], are intriguing systems with a wide range of technological applications [2, 3]. Finite dipole aggregates are expected to display a plethora of nontrivial equilibrium structures due to the competition between the strongly anisotropic dipole–dipole interaction, favoring open, linear structures, and isotropic inter-particle forces, which favor compact structures. In ferrofluids, consisting of a colloidal suspension of magnetite particles, reported observations range from compact and branched macroscopic structures [4] to complex labyrinthine patterns [5, 6], and depend on the applied field. Similar complex structures have been observed in electro-rheological fluids, where electric dipoles are induced by inter-particle interactions [7–9].

Except for aggregates with few particles [3, 10, 11], structural studies of complex fluids have focused on pattern formation in systems with infinitely many particles. Here we present results in the interesting finite-size regime, where the surface energy, favoring compactness, competes with inter-particle interactions, which favor open structures. As the role of the surface diminishes with increasing number of particles, we find the structural motif to evolve from chains and rings to multi-chain and multi-ring assemblies, single- and multi-wall coils, tubes and scrolls. We map the inter-particle interactions in the colloidal suspension onto a continuum model and show how changes in external parameters, such as external magnetic field or the liquid–particle interaction, affect the relative stability of these systems and induce structural transitions.

2. Discrete microscopic model of ferrofluid aggregates

To gain microscopic insight into the causes of pattern formation in ferrofluids, which is beyond the scope of present experimental observations [4, 6], we perform total energy and structure optimization calculations for finite aggregates of magnetic particles suspended in a viscous liquid. Our model system is designed to represent a typical ferrofluid that contains magnetite particles, covered with surfactants, such as oleic acid. These surfactants cause a short-range entropic inter-particle repulsion, which keeps the particles in suspension and prevents a structural collapse. Not only the dynamics of the ferrofluid, but also the effective inter-particle interaction energy is affected by the viscous liquid used in the colloidal suspension, usually *n*-eicosane or kerosene.

The potential energy $U_{\rm tot}$ of magnetic particles with magnetic moment $\boldsymbol{\mu}_i = \mu_0 \hat{\boldsymbol{\mu}}_i$,[4] exposed to an external magnetic field $\boldsymbol{H}$, consists of the potential energy of each particle in the field and pairwise interaction between the particles, as

$$U_{\rm tot} = -\mu_0 \sum_i \hat{\boldsymbol{\mu}}_i \cdot \boldsymbol{H} + \sum_{j>i} (u_{ij}^{\rm dd} + u_{ij}^{\rm nm}). \quad (1)$$

The dipole–dipole interaction $u_{ij}^{\rm dd}$ between two identical particles, separated by $\boldsymbol{r}_{ij} = \boldsymbol{r}_j - \boldsymbol{r}_i$, has the classical form [12]

$$u_{ij}^{\rm dd} = (\mu_0^2/r_{ij}^3)[\hat{\boldsymbol{\mu}}_i \cdot \hat{\boldsymbol{\mu}}_j - 3(\hat{\boldsymbol{\mu}}_i \cdot \hat{\boldsymbol{r}}_{ij})(\hat{\boldsymbol{\mu}}_j \cdot \hat{\boldsymbol{r}}_{ij})]. \quad (2)$$

Following previous work [3, 10, 13], we have described the nonmagnetic part of the inter-particle interaction $u_{ij}^{\rm nm} = u^{\rm nm}(r_{ij})$ by an isotropic potential with a soft-core short-range repulsion and a weak, long-range attraction, with the functional form

$$u_{ij}^{\rm nm} = \epsilon \left[\exp\left(\frac{\sigma - r_{ij}}{\rho_1} \right) - \exp\left(\frac{\sigma - r_{ij}}{\rho_2} \right) \right]. \quad (3)$$

The universal expressions (1)–(3) are well suited to describe typical ferrofluids containing magnetite particles with a magnetic moment of $\mu_0 = 2.1 \times 10^4\ \mu_{\rm B}$. The nonmagnetic interaction between these particles is well represented by the parameters $\rho_1 = 0.25$ nm, $\rho_2 = 0.5$ nm, $\sigma = 10.0$ nm, and $\epsilon = 8$ meV. Our general conclusions about structural arrangements are independent of these particular parameters.

In the following, we first consider the case $H = 0$. In systems with negligible magnetic interactions, particles aggregate to compact, spherical clusters with a near-constant equilibrium inter-particle spacing $L_0 \approx \sigma$. Systems with dominating dipole–dipole interaction, on the other hand, favor straight chains of aligned dipoles with the same separation L_0. Independent of size, the equilibrium geometry of such systems should be a compact arrangement of chains subject to some deformation. In the following, we will analyze the evolution of complex geometries in terms of the particular arrangement of aligned, deformed chains of dipoles.

In a straight, $N \to \infty$ membered chain, the potential energy per particle is given by

$$U^c = U_{\rm tot}^c/N \approx -2\zeta(\mu_0^2/L_0^3) + u^{\rm nm}(L_0), \quad (4)$$

where $\zeta = \sum_{n=1}^{\infty} n^{-3} \approx 1.202\,06$. In the following we will discuss deviations from this expression due to the finite size and deformation of the chain, and due to inter-chain interactions in stable structural arrangements.

3. Continuum model of large ferrofluid aggregates

To compare total energies of finite systems with very many particles and to make universal conclusions about structural transitions, we introduce a continuum model that describes the essence of the dominant interactions. Each chain of $N_{\rm d}$ aligned dipoles of size L_0, illustrated in figure 1(a), is represented by a continuous magnetic rod of diameter[5] d and length L_d. In the following, we will use the number of particles N and the total length $L_d = NL_0$ interchangeably. A planar assembly consisting of $N_{\rm c}$ aligned chains of $N_{\rm d}$ dipoles each, which we consider as a reference structure and show in the left panel of figure 1(b), should thus be $l = N_{\rm c}d$ long and $w = N_{\rm d}L_0$ wide.

The total energy of a system of interacting chains of dipoles, represented by deformed magnetic rods, has three major contributions. The energy required to bend a chain segment of length L_0, depicted in the left panel of figure 1(a), is approximately proportional to the inverse squared radius of curvature R. The same relationship applies for bending a plate to a cylinder, as shown in the middle panel of figure 1(b),

$$\Delta U^{\rm bend} = +\alpha L_0/R^2, \quad (5)$$

albeit with a modified proportionality constant α. This expression may become inaccurate especially for small radii, when deviations from uniform coupling are expected due to the observed fanning alignment of dipoles [14].

The inter-chain interaction energy, associated with cleaving an infinite layer of aligned dipoles along the chain direction, is depicted in the middle panel of figure 1(a). This energy is maximized, when adjacent chains are offset axially by half a unit cell, and is given by

$$\Delta U^{\rm ic} = +\beta L_0. \quad (6)$$

Finally, the energy investment to cleave a straight, infinite chain, illustrated in the right panel of figure 1(a), is a finite constant γ. The energy per chain to cleave an infinite planar assembly of chains normal to the dipole direction is defined in the same way, as

$$\Delta U^{\rm cut} = +\gamma \quad (7)$$

with a modified value of γ. Whereas α and β are rather independent of the size of the plate undergoing a structural change, the value of γ diverges logarithmically with the number of dipoles N in a square plate. Relative stability of arrangements in the particular ferrofluid defined in section 2 are described adequately using $\alpha = \alpha_0 \approx 63.5$ meV nm, $\beta = \beta_0 \approx 1.08$ meV nm^{-1}, and $\gamma(N) = \gamma_0(N) \approx 26.1$ meV $\ln N + 0.887$ meV.

The equilibrium arrangement of dipoles results from the competing tendencies to minimize strain and to maximize inter-particle attraction. A single, straight chain is not strained, but contains two unstable ends. Assemblies of linear chains, shown in the left panels of figures 1(b) and (c), are further stabilized by the pairwise inter-chain interaction. The equilibrium structure represents a compromise between the energy penalty for unterminated chain ends and the energy gain due to inter-chain interaction.

Structures with unterminated chain ends may be stabilized by connecting these ends, which occurs at the expense of increasing strain energy. As shown in the middle panels of

[4] We define $\hat{x} = \mathbf{x}/x$ as the directional unit vector.

[5] Due to the soft-core potential in equation (3), the optimum rod diameter d is slightly larger than its hard-core counterpart $(\sqrt{3}/2)L_0$ in the staggered geometry. For the ferrofluid defined in section 2, the optimum value $d = 8.90$ nm lies close to $(\sqrt{3}/2)L_0 = 8.66$ nm.

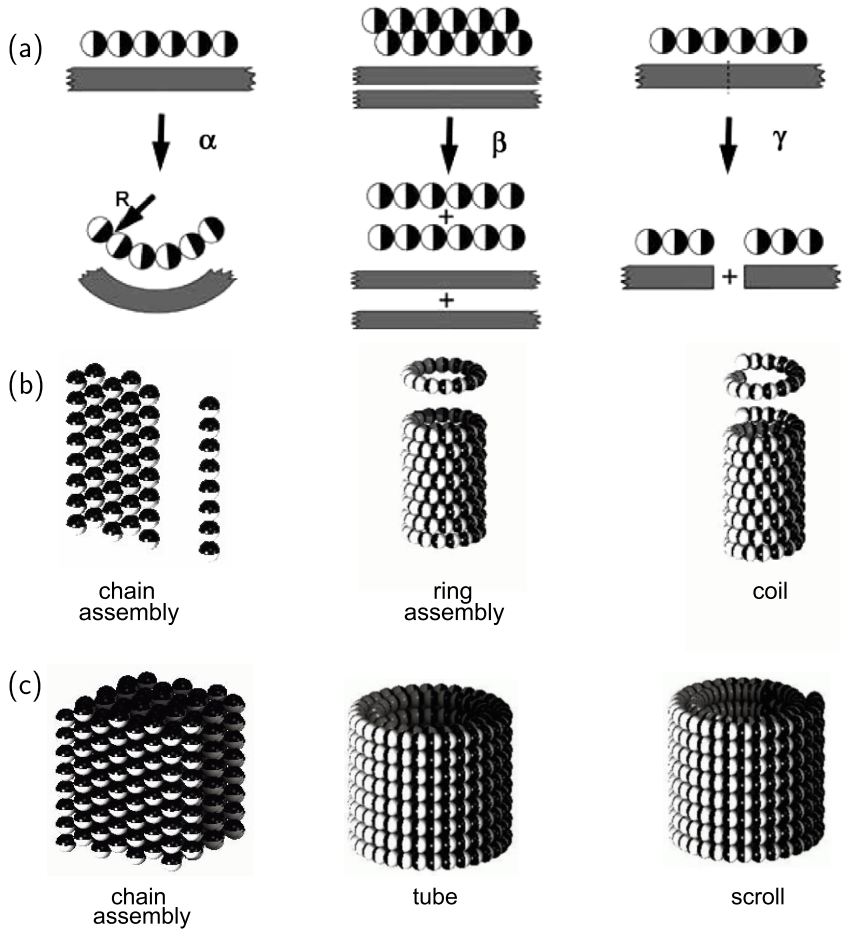

Figure 1. (a) Discrete and continuum models illustrating major energy terms α, β, and γ, associated with structural changes in systems of dipoles. (b) Single-layer structures of dipoles: two-dimensional assembly of chains, assemblies of rings and coils forming single-wall tubes. (c) Multi-layer structures: three-dimensional assembly of chains, multi-wall tubes formed of rings or coils, and scrolls. The orientation of the individual dipoles, depicted as spheres, is represented by the north (black) and south (white) pole hemispheres.

figures 1(b) and (c), assemblies of chains may be deformed to assemblies of rings, which may stack up to form single-wall or multi-wall tubes. In very large systems, where optimizing the inter-chain attraction is more important than avoiding a limited number of chain ends, we may find coils and multi-wall scrolls, shown in the right panels of figures 1(b) and (c), to compete favorably with ring assemblies and multi-wall tubes on energy grounds.

4. Results

To check the accuracy of the continuum approach, we compared the results of the continuum and the discrete description for the two-dimensional structures depicted in figure 1(b). In the continuum approximation, the total energy of a two-dimensional multi-chain assembly of $N = L/L_0$ particles, distributed over N_c parallel chains of equal length, is

$$U^{mc} = +N_c\gamma - \beta L(N_c - 1)/N_c \tag{8}$$

with respect to an N-particle long segment of an infinitely long chain. The corresponding expressions for the energy of a multi-ring assembly and of a coil of radius R are, respectively,

$$U^{mr} = -\beta(L - 2\pi R) + \alpha L/R^2, \tag{9}$$

$$U^{coil} = U^{mr} + \gamma. \tag{10}$$

For a given number of particles N, corresponding to a total chain length L, the optimum number of chain segments N_c in the multi-chain assembly is determined by minimizing $U^{mc}(L, N_c)$ with respect to N_c, yielding

$$N_c^{opt} = (\beta/\gamma)^{1/2} L^{1/2}. \tag{11}$$

In a single-wall tube formed by a multi-ring assembly or a coil, the number of ring turns N_r is given by $N_r = L/(2\pi R)$, and its optimum value is obtained by minimizing the expression in equation (9) with respect to N_r, yielding

$$N_r^{opt} = \left(\frac{\beta}{8\pi^2\alpha}\right)^{1/3} L^{2/3}. \tag{12}$$

For the particular ferrofluid defined in section 2, we compare continuum results, based on equations (11) and (12), to those based on the energy of the discrete system in figures 2(a)

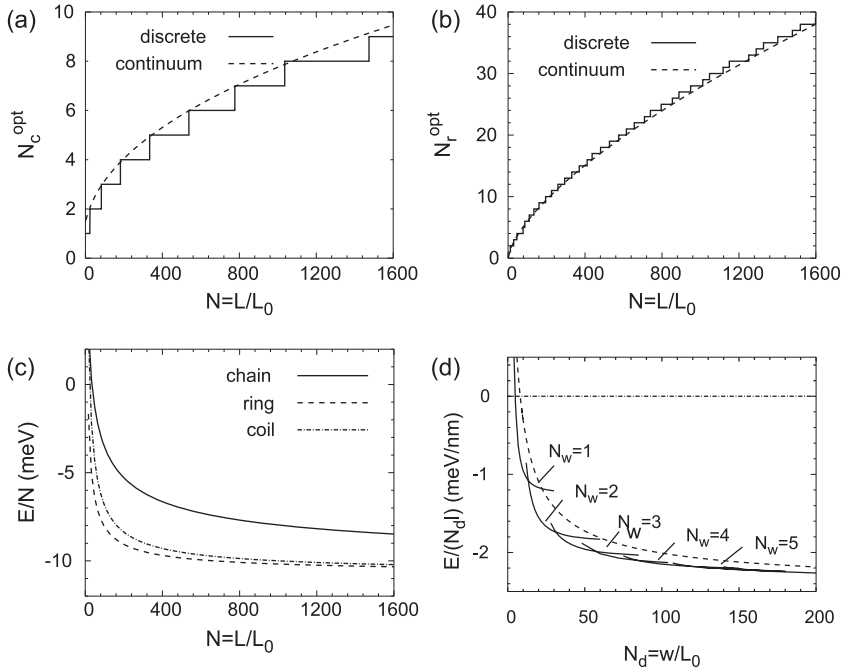

Figure 2. Optimum number of (a) chains, N_c^{opt}, and (b) rings, N_r^{opt}, in single-layer structures of N magnetic dipoles. Optimization results using discrete particles are shown by the solid lines and continuum results by the dashed lines. (c) The energy of optimized chain assemblies, ring assemblies, and coils, as a function of system size $N = L/L_0$, based on the continuum approach. (d) Energy of multi-wall tubes (solid lines) and scrolls (dashed lines) with respect to a reference strip of the same width and length L_d. For sufficiently large N_d values, tubular structures with a growing number of walls N_w are preferred over a planar strip. The higher stability of multi-wall tubes over scrolls results from the absence of exposed edges. All numerical results represent the ferrofluid defined in section 2.

and (b). In view of the fact that N_c^{opt} and N_r^{opt} were not required to be integers in the continuum approach, we find the agreement between the two sets of results very satisfactory, and will base the following discussions on the continuum approach.

For systems with one layer of aligned dipoles, results in figure 2(a) suggest a transition from a single-chain to a double-chain structure for $N > 23$, to a triple-chain structure for $N > 82$, and a planar quadruple-chain assembly for $N > 180$. The extreme aspect ratio or the rectangles is caused by the large energy penalty due to unterminated chains. According to figure 2(b), for a given number of dipoles N, the optimum number of rings in tubular structures exceeds that of chains in planar structures, thus making tubular structures more compact.

Given the optimum geometry of a multi-chain, multi-ring, and a coil assembly, we compare the relative energy per particle of these structures as a function of system size N in figure 2(c). These energy results indicate a transition from a chain to a ring motif for $N > 3$. For systems with $N > 15$ dipoles, the inter-chain attraction more than offsets the bending strain energy, stabilizing coils with respect to planar chain assemblies. Due to the unterminated ends, tubular coil assemblies are always less stable than tubular ring assemblies, with the energy difference decreasing with increasing system size.

The apparent energy preference for coiled or tubular structures suggests this motif for even larger systems. In figure 2(d) we compare the relative stability of single-wall tubes, nested multi-wall tubes, and scrolls. As before, the reference structure is a rectangle consisting of N_c aligned chains, each containing N_d dipoles, yielding an $l = N_c d$ long and $w = N_d L_0$ wide plate. Transforming this structure into a multi-walled nanotube is associated with a strain energy for each component tube, given by equation (5). Same as the inter-chain distance within the plate, we use $\Delta R = \sigma\sqrt{3}/2$ for the inter-wall distance in a multi-wall structure. In sufficiently large systems, the strain energy in bending the plate to cylinders is offset by the inter-wall attraction, which is proportional to all the surface areas of nested tubes.

The energy associated with forming a multi-wall tubular structure from a rectangular plate is thus given by

$$\Delta U^{\text{tube}}/l = \frac{2\pi\alpha}{\Delta R}\sum_{n=1}^{N_w}\frac{1}{R_n} - \frac{\beta}{\Delta R}(2w - \pi(R_{\text{in}} + R_{\text{out}})), \quad (13)$$

where the summation extends over the walls and l is the axial length of the multi-wall tube. R_{in} the radius of the innermost and R_{out} that of the outermost wall, and N_w is the total number of walls.

Unlike a multi-wall tube, which can be decomposed into individual tubes of radius R_n, a scroll structure is contiguous, with the radius $R(\theta)$ a function of the winding angle θ. This fact, and the presence of two exposed edges, modifies the expression for the formation energy of a scroll from a rectangular plate to

$$U^{\text{scroll}}/l = \frac{2\pi\alpha}{(\Delta R)^2}\ln\left(\frac{R_{\text{out}}}{R_{\text{in}}}\right) - \frac{\beta}{\Delta R}(2w - \pi(R_{\text{in}} + R_{\text{out}})) + \frac{\gamma}{\Delta R}. \quad (14)$$

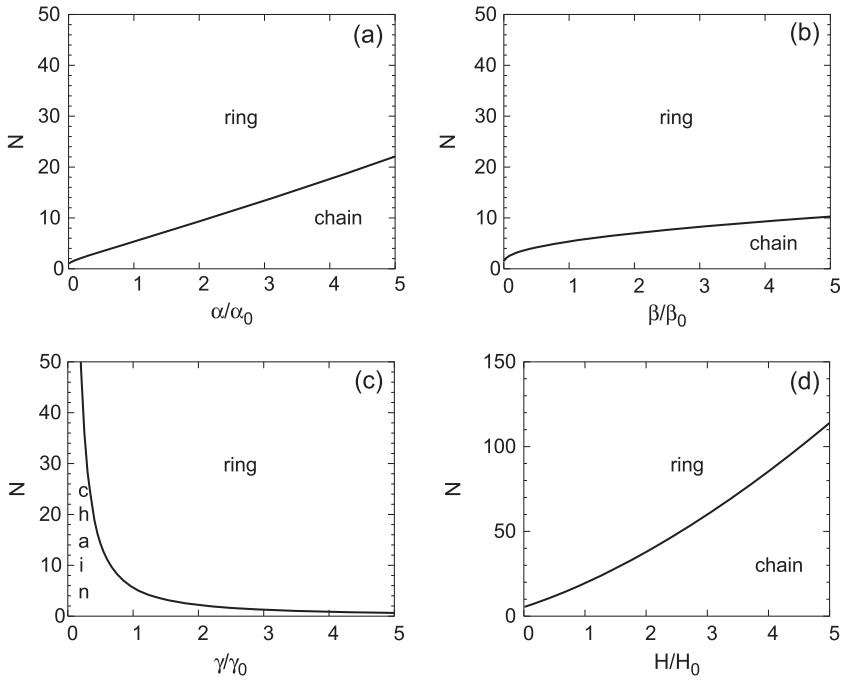

Figure 3. Effect of the parameters α, β, and γ, as well as and external magnetic field H, on the chain-to-ring transition of ferrofluid aggregates. The reference values α_0, β_0, and γ_0 are defined in the text. We use the reference magnetic field $H_0 = 10$ meV$/\mu_0 = 82.27$ G in (d).

Similar to biological systems, where the shape is determined by the presence of hydrophilic or hydrophobic groups, also the structure of ferrofluid aggregates depends sensitively on the interaction between the surfactant and the immersing medium. The effect of this interaction, which also changes the surface energy of the aggregates, is to modify the interaction parameters α, β, and γ with respect to the numerical reference values α_0, β_0, and γ_0, which we provided above for an oleic acid surfactant and kerosene as suspending medium. In figures 3(a)–(c) we show, how changing these parameters affects the critical size for a chain-to-ring transition. The energy penalty γ for unterminated chains plays the most important role, with small γ values favoring large, branched structures, and large γ values favoring compactness. Whereas the chain rigidity α changes the critical size for the chain-to-ring transition linearly as expected, the effect of the inter-chain attraction β on this transition is only secondary.

It is interesting to note that presence of a weak external magnetic field changes the total energy of chain structures as

$$U^{\rm mc}(H) = U^{\rm mc}(H=0) - H\mu_0 L/L_0, \qquad (15)$$

but does not modify the energy of other structures including rings, coils, and tubes[6]. Whereas chain assemblies align with the magnetic field, no such reorientation is expected in those structures with a negligible total magnetic moment. The field-induced stability enhancement of chains with respect to rings increases the critical system size for a chain-to-ring transition, as seen in figure 3(d).

[6] We consider here the case of the dipole–dipole interaction dominating over the field–dipole interaction. In this case, the orientation of individual dipoles is not affected by the external field.

Finally, our theoretical results may give insight into experimental data performed during solidification of ferrofluid aggregates at temperatures, where thermal fluctuations become negligible in comparison to inter-particle interactions. For a given number of particles N, the structural transition from ring to chain occurs at a magnetic field strength of $H_{\rm C}(N)$, thus the total magnetic moment changes from 0 to $N\mu$ for $H \geqslant H_{\rm C}$. Therefore, the magnetic susceptibility should peak at $H_{\rm C}$. This susceptibility peak broadens with increasing temperature and changes its position with changing particle concentration [15].

Except where mentioned specifically, our results are rather general. For a particular system, the appropriate system parameters introduced in this study can be extracted from systematic experiments. The structural phase diagram we found could help to experimentally control the aggregation of magnetic particles. Further theoretical efforts are needed in order to incorporate temperature effects [16] and kinetic components in our model.

5. Summary and conclusions

We studied the equilibrium structure of large but finite aggregates of magnetic dipoles, representing a colloidal suspension of magnetite particles in a ferrofluid. We found that with increasing system size, the structural motif evolves from chains and rings to multi-chain and multi-ring assemblies. Very large systems form single- and multi-wall coils, tubes and scrolls. These structural changes result from a competition between energy terms associated with modifying a reference structure and can be described analytically within a continuum approximation. Analytical expressions, based on

the continuum model, provide universal results also for the effect of the surfactant, the suspending liquid, and an external magnetic field on the equilibrium structure of these aggregates.

Acknowledgments

This work has been funded by the National Science Foundation Cooperative Agreement #EEC-0832785, titled 'NSEC: Center for High-rate Nanomanufacturing'. Computational resources have been provided by the Michigan State University High Performance Computing Center. MY is sponsored by the Materials Science and Engineering Division, Office of Basic Energy Sciences, US Department of Energy (Grant No. ERKCS81) and the Max Planck Society, Germany. We acknowledge useful discussions with Savas Berber and the research group of Weili Luo.

References

[1] Zhang H and Widom M 1994 *Phys. Rev.* E **49** R3591
[2] Raj K, Moshowitz B and Casciari R 1995 *J. Magn. Magn. Mater.* **149** 174
[3] Yoon M, Bormann P and Tománek D 2007 *J. Phys.: Condens. Matter* **19** 086210
[4] Wang H, Zhu Y, Boyd C, Luo W, Cebers A and Rosensweig R E 1994 *Phys. Rev. Lett.* **72** 1929
[5] Dickstein A J, Erramilli S, Goldstein R E, Jackson D P and Langer S A 1993 *Science* **261** 1012
[6] Hong C Y, Jang I J, Horng H E, Hsu C J, Yao Y D and Yang H C 1997 *J. Appl. Phys.* **81** 4275
[7] Wei D and Patey G N 1992 *Phys. Rev. Lett.* **68** 2043
[8] Tao R and Sun J M 1991 *Phys. Rev. Lett.* **67** 398
[9] Klingenberg D J, van Swol F and Zukoski C F 1989 *J. Chem. Phys.* **91** 7888
[10] Jund P, Kim S G, Tománek D and Hetherington J 1995 *Phys. Rev. Lett.* **74** 3049
[11] Clarke A S and Patey G N 1994 *J. Chem. Phys.* **100** 2213
[12] Jackson J D 1975 *Classical Electrodynamics* 2nd edn (New York: Wiley)
[13] Tejero C F, Daanoun A, Lekkerkerker H N W and Baus M 1994 *Phys. Rev. Lett.* **73** 752
[14] Castro L L, Goncalves G R R, Skeff Neto K, Morais P C, Bakuzis A F and Miotto R 2008 *Phys. Rev.* E **78** 061507
[15] El-Hilo M, O'Grady K and Chantrell R W 1992 *J. Magn. Magn. Mater.* **114** 295
[16] Morais P C, Goncalves G R R, Bakuzis A F, Skeff Neto K and Pelegrini F 2001 *J. Magn. Magn. Mater.* **225** 84